ESTIMATION OF UNCERTAINTIES IN TIME ERROR ESTIMATION

Francois Vernotte
Observatoire de Besançon - UPRESA CNRS 6091
41 bis av. de l'Observatoire, BP 1615, F-25010 Besançon Cédex, France
Tel. +33-3-81.66.69.22; Fax +33-3-81.66.69.44
E-mail: francois@obs-besancon.fr

Jérôme Delporte, Michel Brunet, Thierry Tournier
Centre National d'Études Spatiales
18 avenue Edouard Belin, F-31401 Toulouse Cédex 4, France

Abstract

In navigation satellite systems, it is necessary to determine the difference between the on-board time and the reference time for each satellite. This offset can be estimated in real time by filtering time measurements collected over a ground station network, and has to be extrapolated when the satellite is out of visibility of this network. This analysis has been carried out at the CNES in the GNSS2 and GALILEO context and leads to specifications on adjustment and extrapolation errors of the on-board time.

The purpose of this paper is the estimation of the difference between the extrapolation and the real on-board time.

After the description of the method, an example is given using real data, and the predicted extrapolation uncertainties are compared to the real extrapolation errors.

INTRODUCTION

In 1998, CNES proposed a new concept of orbit determination and synchronization for navigation satellite systems [1]. In this architecture, an on-board filter processes measurements collected over a dedicated ground station network and uploaded in quasi real-time, in order to compute the ephemeris and the on-board synchronization. When the satellite is out of visibility from the ground station network, this synchronization has to be predicted. The maximum duration of extrapolation is 3.5 hours with the station network considered by CNES.

In order to estimate the time error of the on-board oscillator when the satellite is hidden, a parabolic fit is performed over the sequence of observed time error data, and extrapolated during the hidden sequence.

The needs of orbit determination and synchronization were specified as the maximum deviation of the time error from the extrapolated parabola. The question is then: how is this maximum deviation related to the noise levels of the oscillator? Several papers have already addressed this question [2] [3] [4], but a new approach was chosen here because we are not only interested in the asymptotic trend of this maximum deviation, but also in its evolution close to the interpolated sequence.

In this paper, we will denote by "Time Interval Error" (TIE) the difference between the extrapolated parabola and the real time error $x(t)$ (seeFigure 1, left). By definition, the TIE samples are then the residuals to this parabola (seeFigure 1, right).

The TIE is due to two effects: the error of determination of the parabola parameters and the error due the noise of the oscillator. Obviously, both of these errors may be positive or negative, and the ensemble average of the TIE is equal to zero (see Figure 2, left). Moreover, it can be easily shown that the ensemble statistics of the TIEare Gaussian (see figure 2, right). Consequently, we only have to estimate the variance of the TIE in order to completely define its statistical characteristics.

Moreover, the removal of a quadratic fit from the time error sequence cancels out the non-stationarity problem of very low frequency noises (see the moment condition in [5]), and the variance of the TIE (i.e. the "true variance") converges for all types of noise without considering a hypothetic low cut-off frequency.

In order to determine an estimation of the TIE, we will first redefine the interpolation method. Then we will compare the equations giving the theoretical estimates of the variance of the TIE to simulations and to real data.

INTERPOLATION METHOD

Interpolating Functions

Let us consider a sequence of N time error data $x(t)$, regularly spaced with a sampling period τ_0: $\{x(t_0), x(t_1), \ldots, x(t_{N-1})\}$, and $t_i = i\tau_0$.

Rather than carrying out a classical quadratic least squares interpolation:

$$x(t) = C_0 + C_1 t + C_2 t^2 + e(t) \tag{1}$$

where $e(t)$ is the noise, i.e. the purely random behavior of $x(t)$, we use the first three Tchebytchev polynomials [5] [6] as interpolating functions (seeFigure 3):

$$\begin{cases} \Phi_0(t) = \dfrac{1}{\sqrt{N}} \\ \Phi_1(t) = \sqrt{\dfrac{3}{(N-1)N(N+1)}}\left[2\dfrac{t}{\tau_0} - (N-1)\right] \\ \Phi_2(t) = \sqrt{\dfrac{5}{(N-2)(N-1)N(N+1)(N+2)}}\left[6\dfrac{t^2}{\tau_0^2} - 6(N-1)\dfrac{t}{\tau_0} + (N-2)(N-1)\right]. \end{cases} \tag{2}$$

The interpolation we use is then:

$$x(t) = P_0\Phi_0(t) + P_1\Phi_1(t) + P_2\Phi_2(t) + e(t). \tag{3}$$

where the parameters $\{P_0, P_1, P_2\}$ have the same dimension as $x(t)$, i.e. time.

The classical parameters $\{C_0, C_1, C_2\}$ of (1) may be easily deduced from the parameters $\{P_0, P_1, P_2\}$ of (3).

Besides their dimensionless nature, the advantage of using these interpolating functions stems from their normality and orthogonality, which greatly simplify the estimation of the parameters P_0, P_1,and P_2,as well as their statistical characteristics, as will be shown. Moreover, the Tchebytchev polynomials minimize the truncation errors, because their covariance matrix is optimized for avoiding bad conditioning problems.

Properties of the Interpolating Functions

Let us define the vector $\vec{\Phi}_i$ associated to the interpolating function $\Phi_i(t)$ as:

$$\vec{\Phi}_i = \begin{pmatrix} \Phi_i(t_0) \\ \vdots \\ \Phi_i(t_{N-1}) \end{pmatrix}. \tag{4}$$

It is then possible to build the matrix $[\Phi]$:

$$[\Phi] = \begin{pmatrix} \vec{\Phi}_0 & \vec{\Phi}_1 & \vec{\Phi}_2 \end{pmatrix} = \begin{pmatrix} \Phi_0(t_0) & \Phi_1(t_0) & \Phi_2(t_0) \\ \vdots & \vdots & \vdots \\ \Phi_0(t_{N-1}) & \Phi_1(t_{N-1}) & \Phi_2(t_{N-1}) \end{pmatrix}. \tag{5}$$

One of the main properties of the Tchebytchev polynomials lies in the orthonormality of the vectors associated to these interpolating functions:

$$[\Phi]^T[\Phi] = [I_3] \tag{6}$$

where $[I_3]$ is the unit matrix (3×3).

Estimation of the Parameters $\{P_0, P_1, P_2\}$

Let us define the vector $\vec{X}$ as:

$$\vec{X} = \begin{pmatrix} x(t_0) \\ \vdots \\ x(t_{N-1}) \end{pmatrix}. \tag{7}$$

This vector may be modeled by:

$$\vec{X} = [\Phi]\vec{P} + \vec{E} \tag{8}$$

where $\vec{P}$ is the vector whose components are the three parameters we want to estimate, and $\vec{E}$ the vector containing the purely random part of $\vec{X}$:

$$\vec{P} = \begin{pmatrix} P_0 \\ P_1 \\ P_2 \end{pmatrix} \quad \text{and} \quad \vec{E} = \begin{pmatrix} e(t_0) \\ \vdots \\ e(t_{N-1}) \end{pmatrix}. \tag{9}$$

In order to estimate $\vec{P}$, we have to calculate:

$$[\Phi]^T\vec{X} = [\Phi]^T[\Phi]\vec{P} + [\Phi]^T\vec{E}. \tag{10}$$

From Equation (6) and because the ensemble average $\left\langle [\Phi]^T \vec{E} \right\rangle = 0$, an estimator of $\vec{P}$ is $\hat{\vec{P}}$ defined by:

$$\hat{\vec{P}} = [\Phi]^T \vec{X}. \tag{11}$$

Thus, the estimate $\hat{P}_j$ of the parameter P_j is easily obtained by calculating:

$$\hat{P}_j = \vec{\Phi}_j^T \cdot \vec{X} = \sum_{i=0}^{N-1} \Phi_j(t_i) x(t_i). \tag{12}$$

ESTIMATION OF THE TIME INTERVAL ERROR (TIE)

Estimation of the Residuals

From (11), the residuals may be defined as a vector $\vec{R}$:

$$\vec{R} = \vec{X} - [\phi]\hat{\vec{P}}. \tag{13}$$

The variance of the residuals σ_e^2 may be estimated by:

$$\sigma_e^2 = \frac{1}{N} \left\langle \vec{R}^T \cdot \vec{R} \right\rangle. \tag{14}$$

From (13) and because the ensemble average $\left\langle \vec{R}^T [\phi] \hat{\vec{P}} \right\rangle = 0$:

$$\left\langle \vec{R}^T \cdot \vec{R} \right\rangle = \left\langle \vec{X}^T \vec{X} \right\rangle - \left\langle \hat{\vec{P}}^T \hat{\vec{P}} \right\rangle. \tag{15}$$

The scalar product $\left\langle \vec{X}^T \vec{X} \right\rangle$ is N times the variance σ_X^2 of the $x(t)$ data and the scalar product $\left\langle \hat{\vec{P}}^T \hat{\vec{P}} \right\rangle$ is the sum of the variances of each estimate $\hat{P}_0$, $\hat{P}_1$, and $\hat{P}_2$. Thus, the variance of the residuals may be estimated by:

$$\sigma_e^2 = \sigma_X^2 - \frac{1}{N} \left(\sigma_{\hat{P}_0}^2 + \sigma_{\hat{P}_1}^2 + \sigma_{\hat{P}_2}^2 \right). \tag{16}$$

Correlation of the Samples

Obviously, the long-term behavior of the TIE depends greatly on the type of noise (from f^{-4} PM to white PM). The autocorrelation function $R_x(t)$ of the $x(t)$ data contains the information about the type of noise. Since it is the Fourier transform of the spectral density $S_x(f)$, $R_x(t)$ may be estimated by using:

$$R_x(t) = 2 \int_{f_l}^{f_h} \cos(2\pi f t) S_x(f) df \tag{17}$$

where f_l is the low cut-off frequency and f_h the high cut-off frequency.

Calculation of the TIE

By hypothesis, we consider that the TIE is the difference between the true time error $x(t)$ at time t, and the extrapolation of the parabola (previously estimated from t_0 to t_{N-1}) up to this time $t > t_{N-1}$:

$$\mathrm{TIE(t)} = \mathrm{x(t)} - \hat{\mathrm{P}}_0\Phi_0(\mathrm{t}) - \hat{\mathrm{P}}_1\Phi_1(\mathrm{t}) - \hat{\mathrm{P}}_2\Phi_2(\mathrm{t}) \qquad \text{and} \quad \mathrm{t} > \mathrm{t_{N-1}}. \tag{18}$$

Thus, the quadratic ensemble average of the TIE may be estimated by:

$$\begin{aligned}\langle \mathrm{TIE}^2(\mathrm{t})\rangle \;=\; & \langle x^2(t)\rangle + \left\langle \hat{P}_0^2 \right\rangle \Phi_0^2(t) + \left\langle \hat{P}_1^2 \right\rangle \Phi_1^2(t) + \left\langle \hat{P}_2^2 \right\rangle \Phi_2^2(t) \\ & -2\left[\left\langle x(t)\hat{P}_0 \right\rangle \Phi_0(t) + \left\langle x(t)\hat{P}_1 \right\rangle \Phi_1(t) + \left\langle x(t)\hat{P}_2 \right\rangle \Phi_2(t)\right] \\ & +2\left[\left\langle \hat{P}_0\hat{P}_1 \right\rangle \Phi_0(t)\Phi_1(t) + \left\langle \hat{P}_0\hat{P}_2 \right\rangle \Phi_0(t)\Phi_2(t) + \left\langle \hat{P}_1\hat{P}_2 \right\rangle \Phi_1(t)\Phi_2(t)\right]. \end{aligned} \tag{19}$$

Consequently, for each type of noise, we have to know: $\langle x^2(t)\rangle = R_x(t)$, the autocorrelation function of $x(t)$; the 3 variances $\left\langle \hat{P}_i^2 \right\rangle = \sigma_{P_i}^2$; the 3 covariances $\left\langle \hat{P}_i\hat{P}_j \right\rangle = \mathrm{Cov(P_i, P_j)}$; and the 3 covariances $\left\langle x(t)\hat{P}_i \right\rangle = \mathrm{Cov\,(x(t), P_i)}$.

RESULTS AND DISCUSSION

Theoretical Results

Since we are interested in the long-term behavior of oscillators, we only estimate the TIE for the 3 lower frequency noises: white FM, flicker FM, and random-walk FM. The theoretical calculation of the above quantities yields the following variance:

- White FM:

$$\langle TIE^2(t)\rangle \approx \frac{6\pi^2 k_{-2}\tau_0}{35N^3}\left(50\frac{t^4}{\tau_0^4} - 100N\frac{t^3}{\tau_0^3} + 69N^2\frac{t^2}{\tau_0^2} - 19N^3\frac{t}{\tau_0} + N^4\right). \tag{20}$$

- Flicker FM:

$$\begin{aligned}\langle TIE^2(t)\rangle \;\approx\; & \frac{\pi^2 k_{-3}\tau_0^2}{8N^2}\left[\frac{192}{N^2}\frac{t^6}{\tau_0^6} - \frac{576}{N}\frac{t^5}{\tau_0^5} + 692\frac{t^4}{\tau_0^4} - 424N\frac{t^3}{\tau_0^3} + 136N^2\frac{t^2}{\tau_0^2} - 20N^3\frac{t}{\tau_0} + N^4\right. \\ & \left. + \frac{96}{N^3}\frac{t^3}{\tau_0^3}\ln\left(1 - \frac{N\tau_0}{t}\right)\left(2\frac{t^4}{\tau_0^4} - 7N\frac{t^3}{\tau_0^3} + 9N^2\frac{t^2}{\tau_0^2} - 5N^3\frac{t}{\tau_0} + N^4\right)\right]. \end{aligned} \tag{21}$$

- Random walk FM:

$$\langle TIE^2(t)\rangle \approx \frac{2\pi^4 k_{-4}\tau_0^3}{315N}\left(450\frac{t^4}{\tau_0^4} - 1110N\frac{t^3}{\tau_0^3} + 933N^2\frac{t^2}{\tau_0^2} - 294N^3\frac{t}{\tau_0} + 23N^4\right). \tag{22}$$

All the above equations were obtained under the assumption $N \gg 1$.

Estimation of the TIE Using the Variance of the Residuals

The relationships (20) to (22) need an explicit knowledge of the noise levels k_α. However, for very long-term interpolation (several days), we may be sure of the dominant

type of noise: the flicker FM for a cesium clock or the random-walk FM for a quartz oscillator.

Thus, the variance of the TIE may be estimated directly from the variance of the residuals :

- Flicker FM: from (16) we obtain

$$\sigma_e^2 \approx \frac{\pi^2 N^2 k_{-3} \tau_0^2}{24} \tag{23}$$

and from (21) and (23):

$$\begin{aligned}\langle TIE^2(t) \rangle \approx \frac{3\sigma_e^2}{N^4} \Bigg[& \frac{192}{N^2}\frac{t^6}{\tau_0^6} - \frac{576}{N}\frac{t^5}{\tau_0^5} + 692\frac{t^4}{\tau_0^4} - 424N\frac{t^3}{\tau_0^3} + 136N^2\frac{t^2}{\tau_0^2} - 20N^3\frac{t}{\tau_0} + N^4 \\ & + \frac{96}{N^3}\frac{t^3}{\tau_0^3} \ln\left(1 - \frac{N\tau_0}{t}\right)\left(2\frac{t^4}{\tau_0^4} - 7N\frac{t^3}{\tau_0^3} + 9N^2\frac{t^2}{\tau_0^2} - 5N^3\frac{t}{\tau_0} + N^4\right)\Bigg]. \end{aligned} \tag{24}$$

- Random-walk FM: from (16) we obtain

$$\sigma_e^2 \approx \frac{\pi^4 N^3 k_{-4} \tau_0^3}{315} \tag{25}$$

and from (22) and (25):

$$\langle TIE^2(t) \rangle \approx \frac{2\sigma_e^2}{N^4}\left(450\frac{t^4}{\tau_0^4} - 1110N\frac{t^3}{\tau_0^3} + 933N^2\frac{t^2}{\tau_0^2} - 294N^3\frac{t}{\tau_0} + 23N^4\right). \tag{26}$$

It may be noticed that, for a fixed value of σ_e^2, the asymptotic ratio of Equation (26) over Equation (24) is exactly equal to 3 when t tends toward infinity.

However, this method is less precise than the use of a correct estimation of the noise levels, due to the statistics of the estimate of the variance of the residuals. We have observed experimentally that this estimate is χ^2 distributed with a small number of degrees of freedom (3 for a flicker FM and 2 for a random-walk FM). Consequently, the standard deviation of the TIE, i.e. the square root of equations (24) and (26), follows a Student law. Thus, the bounds given by the square root of Equations (24) and (26) still contain 68% of the realizations, but the 95% confidence interval (2σ) is more than 3 times higher.

Comparison with Simulations

In order to verify the Equations (20) to (22), we simulated time error sequences of different types of noise (white FM, flicker FM and random-walk FM). For each type of noise, 10,000 realizations were calculated with the same noise level[1] ($k_{-2} = 1.4 \cdot 10^{-4}$s, $k_{-3} = 3.3 \cdot 10^{-8}$ or $k_{-4} = 5.0 \cdot 10^{-12}$s^{-1}), the same number of data (65,536), the same number of data taken into account for the fit (8640), and the same time of estimation of the TIE ($\frac{t}{\tau_0}$ equals to {8639, 9900, 11350, 13000, 14900, 17000, 19500, 22400, 25700, 29400, 33700, 38600, 44300, 50700, 58100, 65535}). The noise levels were chosen such that the variance of the residuals equals 1.

[1] We denote k_α the noise levels of the time error spectral density $S_x(f)$, and $h_{\alpha+2}$ the corresponding noise levels of the frequency deviation spectral density $S_y(f)$. These coefficients are related by: $h_{\alpha+2} = 4\pi^2 k_\alpha$.

Figure 4 shows the curves corresponding to the square root of equations (20) to (22) compared to the standard deviation estimated from the 10,000 simulations (i.e. half the width of the Gaussian ofFigure 2). The simulations exhibit a quite good agreement with the theoretical curves.

Application to Real Oscillators

Figures 5 to 8 compare the long-term behavior of 2 real quartz oscillators to the bounds given by the estimated standard deviation of the TIE (the square root of equations (20) to (22)).

The data from the oscillators are time errors sampled with a sampling period $\tau_0 = 10$ s. The fit was carried out over the first 24 hours of each sequence and extrapolated over the whole sequence (6 days for oscillator 1 and 90 hours for oscillator 2).

For oscillator 1, the Allan variance yields $h_{-2} = 4 \cdot 10^{-29}$ s^{-1}, i.e. $k_{-4} = 10^{-30}$ s^{-1}. Thus, the bounds ofFigure 5 were obtained by using the square root of (22). On the other hand, the variance of the residuals of the interpolated part (i.e. the first 24 hours) is $\sigma_e^2 = 1,4 \cdot 10^{-17}$ s^2. Thus, the bounds ofFigure 6 were obtained by assuming that the random-walk FM was dominant and by using the square root of (26).

For oscillator 2, the Allan variance revealed that 2 types of noise must be taken into account: white FM ($h_0 = 10^{-22}$ s, i.e. $k_{-2} = 2,5 \cdot 10^{-24}$ s) and random walk FM ($h_{-2} = 1,5 \cdot 10^{-31}$ s^{-1}, i.e. $k_{-4} = 4 \cdot 10^{-33}$ s^{-1}). Thus, the bounds ofFigure 7 were obtained by using the square root of the sum of (20) and (22). On the other hand, the variance of the residuals of the interpolated part (i.e. the first 24 hours) is $\sigma_e^2 = 1,4 \cdot 10^{-18}$ s^2. In this case also, we assumed that the random-walk FM was dominant, and the bounds ofFigure 8 were obtained by using the square root of (26).

The experimental TIE curves remain in the theoretical bounds except for Figure 6. This is quite compatible with the statistics of TIE since 32% of the realizations should be outside the bounds.

CONCLUSION: A New Strategy for Long-Term Stability Analysis

Besides the interest of this method for synchronization prediction, it may also be used for defining a new method for very long-term stability analysis.

An oscillator may be continuously measured during a few days (e.g. a time error measurement with a sampling period of 1 minute during 10 days). From these data, the noise levels of this oscillator could be precisely determined [7] [6] and a quadratic fit could be carried out. Thus, if the oscillator is continuously running in the same conditions, it could be possible to extrapolate the difference of this oscillator with the parabolic fit after a few months or one year.

This analysis could be helpful in low accuracy time keeping applications, for instance for industrialists who periodically send their oscillator to an accreditation laboratory.

REFERENCES

[1] T. Tournier, *"A precise on-board real-time ephemeris and clock estimation for GNSS2 concepts studied at CNES,"* in Proceedings of GNSS 98, October 1998, p. IX-O-12.

[2] L. G. Bernier, *"Linear prediction of the non-stationary clock error function,"* in Proceedings of EFTF 88, March 1988, Neuchâtel, Switzerland, 125-137.

[3] L. Di Piro, E. Perone, and P. Tavella, *"Random walk and first crossing time: applications in metrology,"* in Proceedings of EFTF 98, March 1998, Warsaw, Poland, 388-391.

[4] F. Vernotte, and M. Vincent, *"Estimation of the measurement uncertainty of drift coefficients versus the noise levels,"* in Proceedings of EFTF 98, March 1998, Warsaw, Poland, 222-227.

[5] J. E. Deeter, and P. E. Boynton, *"Techniques for the estimation of red power spectra. I. context and methodology,"* **The Astrophysical Journal, 261**, 337–350.

[6] F. Vernotte, *"Estimation of the Power Spectral Density of Phase: comparison of three methods,"* in Proceedings of EFTF-IFCS 99, April 1999, Besançon, France.

[7] F. Vernotte, E. Lantz, J. Groslambert, and J. Gagnepain, *"Oscillator noise analysis: multivariance measurement,"* **IEEE Trans. on Inst. and Meas., IM-42**, 342–350.

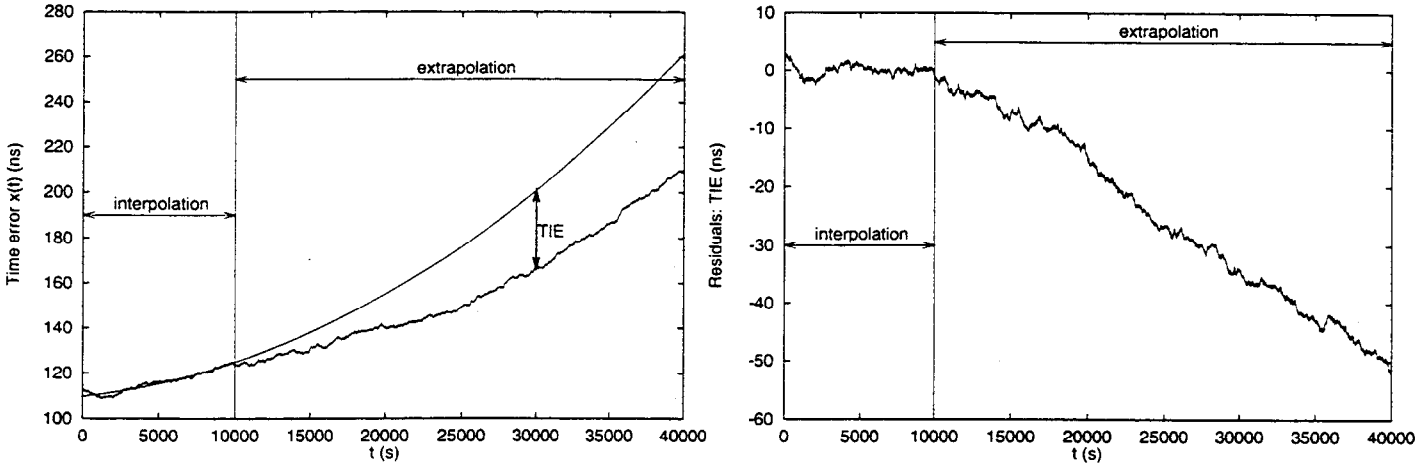

Figure 1: Quadratic fit over a time error sequence of white FM (left). The fit is performed over the first quarter of the sequence. The residuals of this fit (right) correspond to our definition of the TIE.

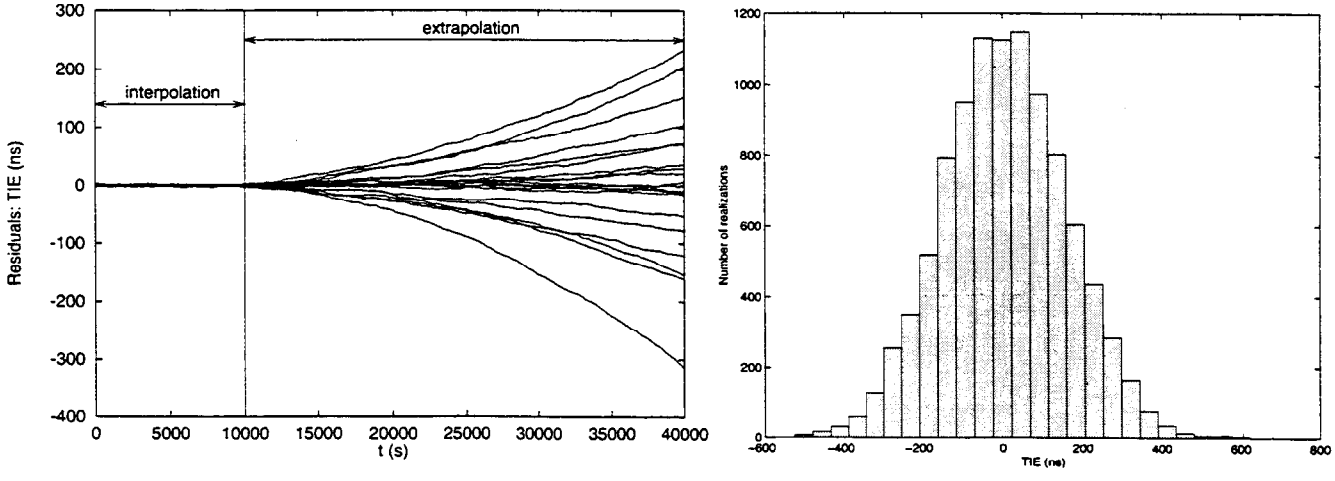

Figure 2: Dispersion of the TIE for 20 realizations of the same white FM process (left). The histogram of 10000 realizations of the TIE estimates (here for $t = 40{,}000$s) exhibits a Gaussian behavior.

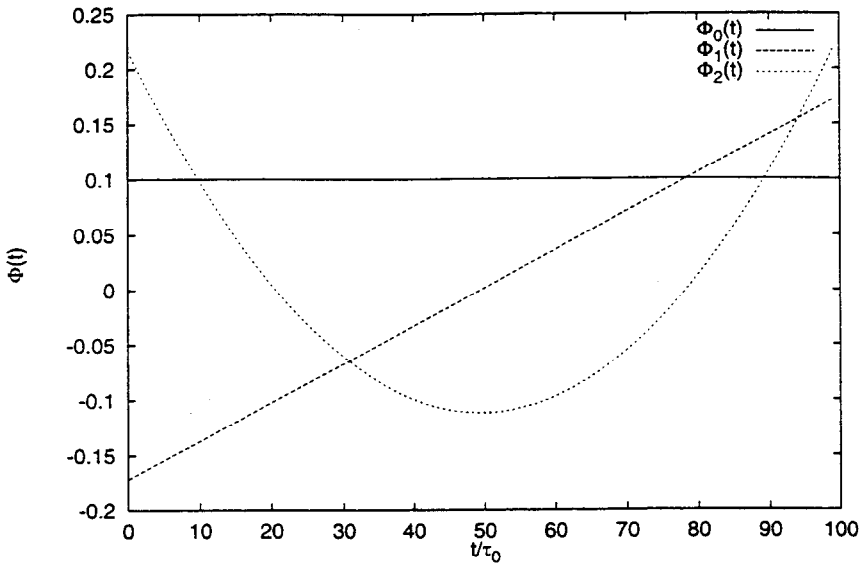

Figure 3: The first 3 Tchebytchev polynomials calculated for $N = 100$ data.

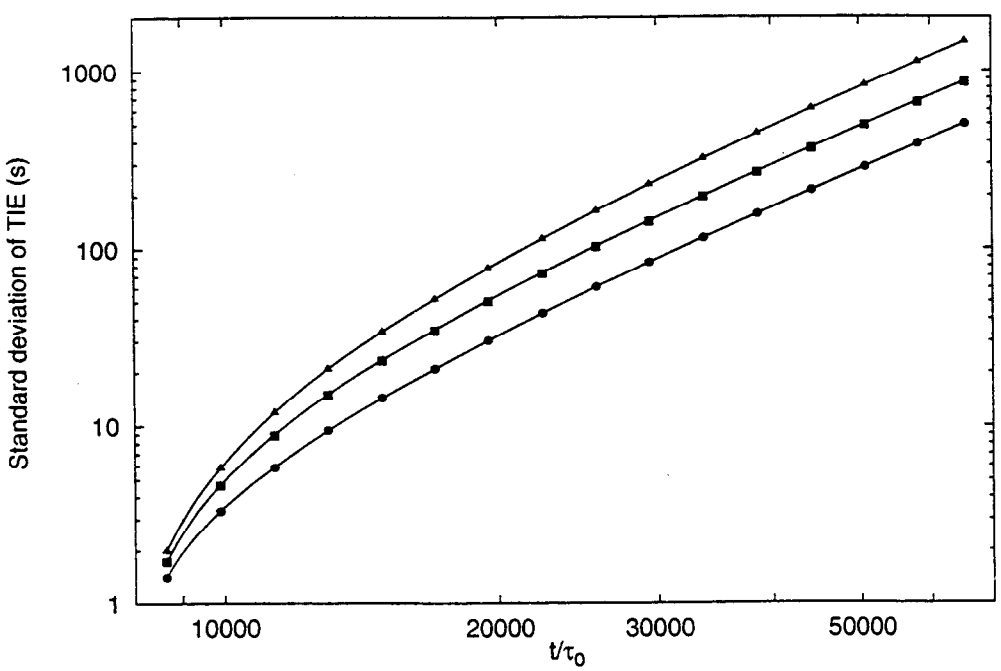

Figure 4: Comparison of the estimation of the standard deviation of the TIE calculated from the equation (20) to (22) (solid lines) and estimated over 10,000 realizations of simulated noise (circles, squares, and triangles). The lower curve was obtained with white FM (circles), the middle one with flicker FM (squares), and the upper one with random walk FM (triangles). In order to use the same scale, the noise levels were defined in such a way that the variance of the residuals is equal to one ($k_{-2} = 1.4 \cdot 10^{-4}$s, $k_{-3} = 3.3 \cdot 10^{-8}$, $k_{-4} = 5.0 \cdot 10^{-12}$s^{-1}). The error bars corresponding to the estimates of the simulated noises are too small to be plotted on this graph.

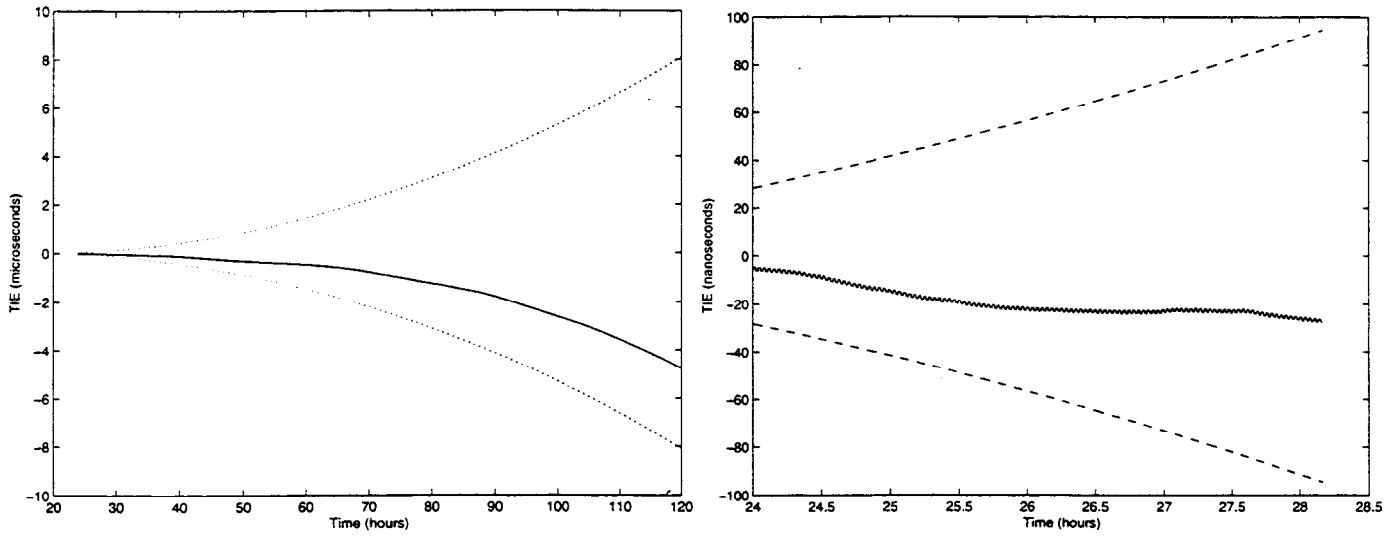

Figure 5: Oscillator 1. Evolution of the TIE after the fitted sequence. The fit was performed over 1 day with a sampling period of 10s. The estimation of the TIE (dashed line) was performed from Equation (22) by using a noise level estimate: $k_{-4} = 10^{-30}\mathrm{s}^{-1}$. On the right, the plot is an enlargement of the first 4 hours.

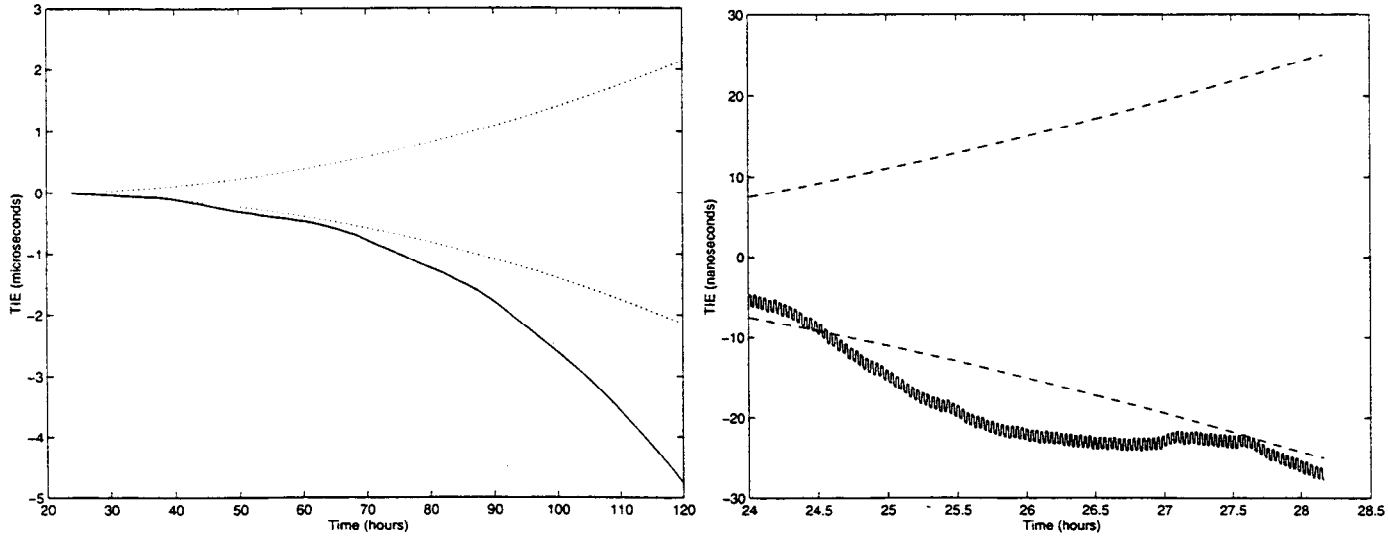

Figure 6: Oscillator 1. Same as fig. 5. The estimation of the TIE (dashed line) was performed from Equation (26) by using the variance estimate of the residuals $\sigma_e^2 = 1,4 \cdot 10^{-17}\ \mathrm{s}^2$. On the right, the plot is an enlargement of the first 4 hours.

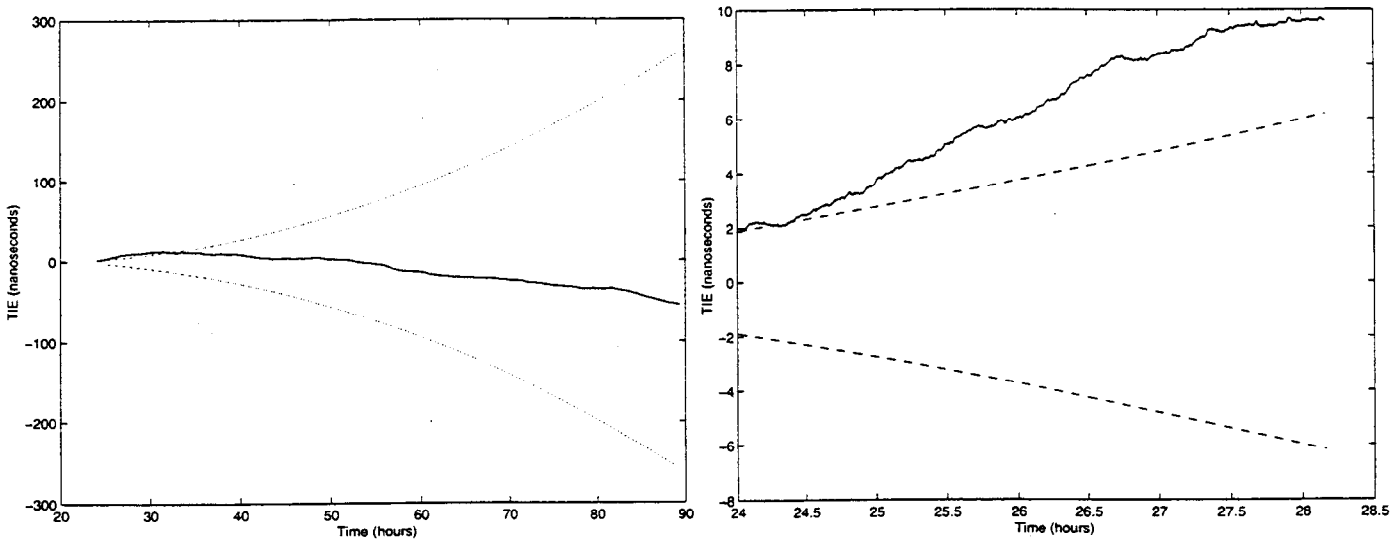

Figure 7: Oscillator 2. Evolution of the TIE after the fitted sequence. The fit was performed over 1 day with a sampling period of 10s. The estimation of the TIE (dashed line) was performed from Equations (20) and (22) by using the noise level estimates: $k_{-2} = 2,5 \cdot 10^{-24}$ s and $k_{-4} = 4 \cdot 10^{-33}$ s^{-1}. On the right, the plot is an enlargement of the first 4 hours.

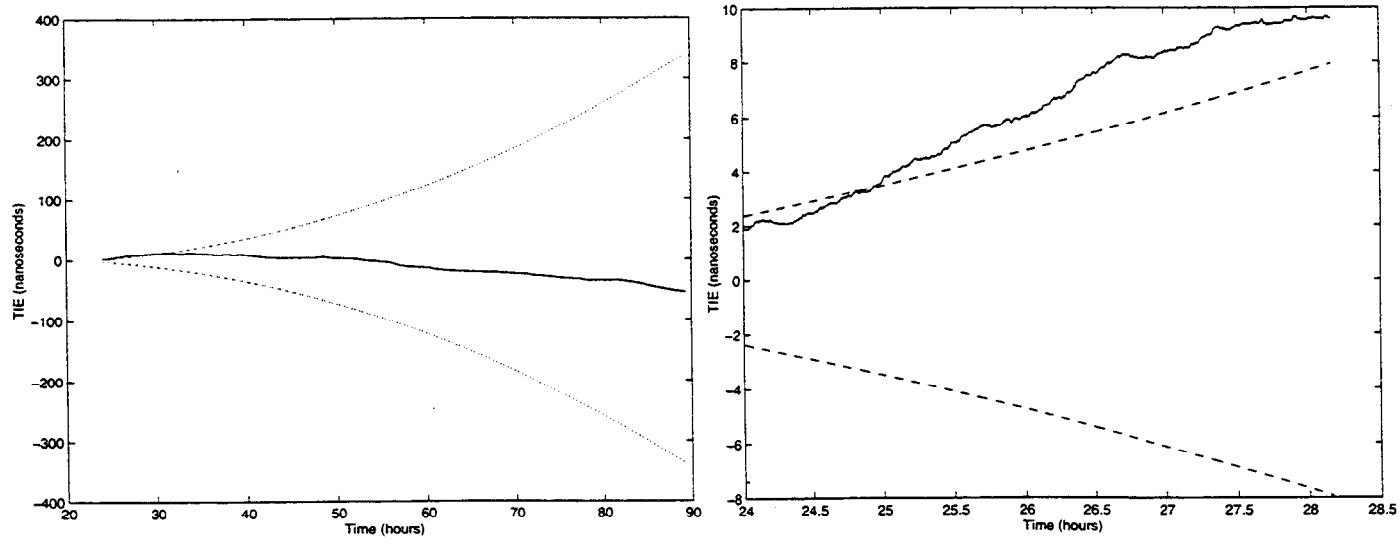

Figure 8: Oscillator 2. Same as fig. 7. The estimation of the TIE (dashed line) was performed from Equation (26) by using the variance estimate of the residuals $\sigma_e^2 = 1,4 \cdot 10^{-18}$ s^2. On the right, the plot is an enlargement of the first 4 hours.